https://doi.org/10.5194/bg-2019-486
Preprint. Discussion started: 29 January 2020

Biogeosciences Discussions

Carbon dioxide dynamics in an agricultural headwater stream driven by hydrology and primary production

Marcus B. Wallin[1]*, Joachim Audet[2], Mike Peacock[3], Erik Sahlée[1], Mattias Winterdahl[1,4,5]

[1]Department of Earth Sciences, Uppsala University, Uppsala, Sweden
[2]Department of Bioscience, Aarhus University, Silkeborg, Denmark
[3]Department of Aquatic Sciences and Assessment, Swedish University of Agricultural Sciences, Uppsala, Sweden
[4]Department of Physical Geography, Stockholm University, Stockholm, Sweden
[5]Bolin Centre for Climate Research, Stockholm, Sweden

Correspondence to: Marcus B. Wallin (marcus.wallin@geo.uu.se)

Abstract. Headwater streams are known to be hotspots for carbon dioxide (CO_2) emissions to the atmosphere and are hence important components in landscape carbon balances. However, surprisingly little is known about stream CO_2 dynamics and emissions in agricultural settings, a land-use type that globally cover ca 40% of the continental area. Here we present continuously measured in-situ CO_2 concentration data from a temperate agricultural headwater stream covering more than one year of open-water season. The stream CO_2 concentrations during the entire study period were generally high (median 3.44 mg C L^{-1}, corresponding to partial pressures (pCO_2) of 4778 µatm) but were also highly variable (IQR = 3.26 mg C L^{-1}). The CO_2 concentration dynamics covered a variety of different time-scales from seasonal to hourly, and with an interplay of hydrological and biological controls. The hydrological control was strong (although with both positive as well as negative influences dependent on season) and CO_2 concentrations changed rapidly in response to rainfall and snowmelt events. However, during growing-season baseflow and receding flow conditions, aquatic primary production seemed to control the stream CO_2 dynamics resulting in elevated diel patterns. Given the observed high levels of CO_2 and its temporally variable nature, agricultural streams clearly need more attention in order to understand and incorporate these considerable dynamics in large scale extrapolations.

1. Introduction

Fluvial systems (streams and rivers) are estimated to dominate the inland water CO_2 source globally, surpassing CO_2 emissions by lakes and reservoirs by a factor of six (Raymond et al. 2013). However, this estimate relies on a number of assumptions and the scarcity of empirical data makes it uncertain. One of the critical gaps in the global upscaling is the lack of direct measurements from agriculture dominated areas (Osborne et al. 2010). Globally, agricultural land covers about 40% of the

https://doi.org/10.5194/bg-2019-486
Preprint. Discussion started: 29 January 2020


Biogeosciences Discussions

total continental area (Ramankutty et al., 2008) but there are few studies specifically focusing on the magnitude and dynamics of CO_2 emissions from agricultural streams. The few studies that do exist conclude that CO_2 concentrations in such streams are generally high and up to five times greater than those in streams draining forested areas which are more extensively studied (Borges et al. 2018; Bodmer et al. 2016; Wallin et al. 2018). For example, Bodmer et al. (2016) measured partial pressure of CO_2 (pCO_2) in German and Polish streams and examined differences between forested and agricultural catchments. They found that pCO_2 was generally 2-3 higher times in agricultural streams compared to streams draining forested areas. Similarly, Borges et al. (2018) found high CO_2 concentrations in streams and rivers dominated by agriculture in the river system Meuse, Belgium. They linked the higher pCO_2 in agricultural streams (up to 5 times higher than in forested areas) to elevated levels of dissolved organic carbon (DOC), particulate organic carbon (POC) and inorganic nitrogen.

There are numerous factors influencing CO_2 patterns in stream systems and often site-specific controls dominate. Hence, large scale generalizations are difficult to make (Crawford et al. 2017). CO_2 concentrations in nutrient-poor forest and peatland streams are often related to variations in stream discharge but with site-specific response patterns, both positive and negative (Crawford et al. 2017; Dinsmore et al. 2013). These response patterns have often been connected to the catchment characteristics and changes in hydrological pathways, which in turn control the dominant CO_2 source areas of catchment soils (Campeau et al. 2018; Leith et al. 2015; Dinsmore and Billett 2008). In contrast, other catchments lack a strong hydrological control and instead display clear diel cycles in the stream CO_2 concentration indicating a metabolic control (Crawford et al. 2017). Here the interplay of photosynthesis and respiration (in-stream or terrestrial) could result in large day to night time differences in stream CO_2. These recent findings concerning dynamics and controls on stream CO_2 concentrations have been possible due to the development of cost-effective CO_2 sensors (e.g. Johnson et al. 2010; Bastviken et al. 2015) which have enabled continuous data collection covering relevant time-scales. However, very little information about stream CO_2 dynamics exists from agricultural areas, a land-use type that is heavily managed by humans from multiple aspects including hydrological drainage, nutrient additions, soil cultivation etc. As a consequence, CO_2 patterns in agricultural streams could potentially be very different than in other land-use types with amplified diel CO_2 dynamics due to high metabolism and/or quicker response to hydrological events due to effective drainage systems.

https://doi.org/10.5194/bg-2019-486
Preprint. Discussion started: 29 January 2020

In addition to the concentration gradient between the stream water and the above air, gas exchange is also highly dependent on the physical conditions at the air-water interface. For stream systems, the gas transfer velocity (often the variable given to describe the efficiency of the air-water gas exchange) is related to a combination of hydrological and morphological conditions of the stream channel, often including slope, velocity and depth (Raymond et al. 2012; Wallin et al. 2011). All these variables are proxies for describing the water turbulence of the stream which controls the gas exchange but that is rarely directly measured (Kokic et al. 2018). Agricultural areas are often located in flat landscapes resulting in drainage systems that are low-gradient and slow-flowing (Rhoads et al. 2003; Hughes et al. 2010), conditions that prevent effective air-water gas exchange (Hall & Ulseth, 2019). However, whether the elevated pCO_2 observed in agricultural streams is an effect of land-use specific hydro-morphological stream conditions preventing efficient gas exchange or an effect of high internal (aquatic) or external (terrestrial) CO_2 production is currently unknown.

Although recent studies have shown the potential importance of agricultural streams, there are still large knowledge gaps to be filled in order to improve our understanding concerning the influence of these waterbodies in landscape C cycling. Here we present high-resolution CO_2 concentration measurements in a Swedish agricultural headwater stream during more than a year of open water season. The study aimed to 1) quantify CO_2 concentration levels in an agricultural stream and explore its temporal dynamics, 2) identify the main drivers causing temporal variability in stream CO_2 concentration and how they might vary with season.

2. Methods

2.1. Study area

The study was conducted within the 11.3 km^2 Sundbromark (SBM) catchment (59°55′N, 17°32′E), located 5 km NW of the city of Uppsala, Sweden (Figure 1). The 30 year (1960-1991) mean annual, January and July temperatures for the area are 5.3°C, -4.5 and 16.0 and with a mean annual precipitation of 535 mm (SMHI). The catchment is dominated by agricultural land (86%) and with minor influence of forest (8%) and urban areas (6%). The area is flat with only 28 m elevation difference from 41 m.a.s.l. at the highest point to 13 m.a.s.l. at the catchment outlet (Table 1). The bedrock consists of gneissic granites

https://doi.org/10.5194/bg-2019-486
Preprint. Discussion started: 29 January 2020

and the soils are dominated by post glacial clay at lower elevations and with some influence of glacial clay and silt at higher elevations. Although the bedrock does not contain any known carbonates, the soils are alkaline due to glacial carbonate containing deposits resulting in a stream pH ranging 7.4-8.4 (Table 2) and with high electrical conductivity (EC, ranging 791-1908 µS cm^{-1}) (Osterman 2018). The nutrient and DOC levels of the stream water (Table 1) are at the lower end of monitored agricultural catchments in Sweden (Linefur et al. 2018; Kyllmar et al. 2014). The oxygen conditions are mainly undersaturated (median D.O. = 53%) during the growing season. The arable fields are to a large extent artificially drained with extensive tile drainage pipe systems connected to the stream network. The catchment is a part of the hydro-meteorological observatory Marsta that was established in the late 1940s (Halldin et al. 1999).

To explore how representative the SBM catchment is for streams draining agricultural areas in the region, a snapshot sampling survey was performed across 10 streams (denoted region UPP 2 in the study by Audet et al. (2019)) of various sizes (catchment area 8.5-740 km^2) and agricultural influence (30-86%) distributed within a radius of 10 km from the city center of Uppsala (Table S1).

2.2. Field sampling and analysis

The measurements were conducted during the open-water season from Sep 26, 2017 to Dec12, 2018. Stream CO_2 concentration was monitored using an EosGP sensor (Eosense, Dartmouth, Canada). The sensor was covered by copper tape in order to avoid biofouling. Sensor accuracy is <1% of the calibrated range (0-2% CO_2) + 1% of the reading corresponding to a maximum error of ca 0.3 mg C L^{-1} based on the maximum CO_2 measured in the current study. The CO_2 sensor was calibrated against known gas standards before and after deployment. No significant drift (exceeding the above given uncertainty) in the instrument was observed during the period. Volume fraction outputs from the sensor were corrected for variations in temperature and pressure (atmospheric and water depth) using the method described in Johnson et al. (2010) and expressed in the unit of mg C L^{-1}. Only CO_2 data measured at discharge rates > 0 L s^{-1} were used in the analysis of the data.

Water level, water temperature and EC were measured together with CO_2 concentration at a V-notch weir. Water level was measured using a pressure transducer (1400, MJK Automation, Sweden) mounted in a stilling well representing the stream

https://doi.org/10.5194/bg-2019-486
Preprint. Discussion started: 29 January 2020

water level at the V-notch weir. Discharge was calculated from a stage-discharge rating curve based on a series of manual measurements and according to a rating curve presented in Holmqvist (1998). Water temperature and EC were monitored using a thermocouple (Type T) and a CS547A-L conductivity sensor (Campbell, UK), respectively. The sensors (except for the pressure transducer) were deployed under the water surface attached to a wooden rod in the center of the stream just upstream of the weir. All sensors were connected to a CR1000X data logger (Campbell, UK) which stored average data (measurements every 1 minute) at a temporal resolution of 30 (in 2017) or 60 (in 2018) minutes.

Stable isotopic analysis of the dissolved inorganic carbon (DIC) (δ^{13}C-DIC) was performed on six occasions during the falling limb of the snowmelt discharge peak in 2018 in order to explore the temporal variability in DIC source. Samples for analysis of δ^{13}C-DIC were taken in a 60 ml glass vial completely filled with stream water and closed airtight with a rubber septum below the water surface. In order to preserve the sample, 1 ml of highly concentrated $ZnCl_2$ solution was injected in each sample (with subsequent release of 1 ml of sample in order to keep atmospheric pressure) directly after sample collection. Samples were kept cold and dark until analysis. Prior to analysis, 2 ml of sample was injected into 12 ml septum-sealed pre-combusted glass vials (Labco Limited) pre-filled with N_2 gas, and pre-injected with 1 ml of phosphoric acid in order to convert all DIC species to CO_2(g) (Campeau et al. 2017a). The samples were analyzed using an isotope ratio mass spectrometer (DeltaV Plus,Thermo Fisher Scientific, Bremen, Germany) Gasbench II (Thermo Fisher Scientific, Bremen, Germany) measuring the CO_2 in the headspace. Each sample was analyzed seven times and the first two injections for each sample were discarded to avoid memory effects, and the mean was taken of the other five to give the final result. The δ^{13}C-DIC values are given in terms of deviation from the standard Pee-Dee Belemnite (PDB) in per mille where R is the isotopic ratio of [^{13}C]/[^{12}C]:

$$\delta^{13}\text{C–DIC (‰)} = (R_{sample}/R_{standard}\text{-}1) \times 1000$$

Precipitation, air temperature and incoming shortwave (global) radiation data (Figure 2) were obtained from the Marsta meteorological observatory located within the catchment ca 2.5 km from the stream sampling station (Halldin et al. 1999). In the absence of direct measurements of photosynthetically active radiation (PAR) shortwave incoming radiation was used as a proxy for available photosynthetic light.

https://doi.org/10.5194/bg-2019-486
Preprint. Discussion started: 29 January 2020

A spatial sampling campaign for CO_2 concentration, pH, EC and water temperature was conducted on June 21, 2018 across ten streams located around the city of Uppsala. The sampling was performed between 10.00 and 14.00 during the day. Samples for CO_2 analysis were collected using the headspace method (Hope et al., 2004; Kokic et al. 2015). Briefly, 30 mL bubble-free water were collected in 60 mL polypropylene syringes and equilibrated with a known volume of ambient air by shaking vigorously for 1 min. The equilibrated headspace (15-20 mL) was recovered and analysed on an Ultraportable Greenhouse Gas Analyzer (UGGA) (Los Gatos Research, USA) equipped with a soda lime filter and manual injection port. In situ CO_2 concentration was calculated from the UGGA-determined ppm values using Henry's law considering stream temperature (Weiss 1974), atmospheric pressure, the added ambient air, as well as the water-air volume ratio in the syringe. pH, EC and water temperature were measured in-situ in the streams with handheld instruments, for pH with a pH110 pH-meter (VWR, USA), and for EC and temperature with a HI 99300 (Hanna Instr., USA).

2.3. Delineation of the stream network and catchment characteristics

Catchment area and characteristics were calculated in QGIS 3.8 based on a high resolution (2×2 m) digital elevation model (DEM) derived from LIDAR data (GSD Elevation data, grid 2+, Swedish Land Survey). Land use distribution within the catchment was derived from the CORINE Land Cover 2018 product (European Environment Agency), and soil and bedrock characteristics were based on digital versions of the Quaternary deposits (1:25,000 – 1:100,000) and bedrock (1:50,000 – 1:250,000) maps (Swedish Geological Survey).

2.4. Data analysis

The continuous data from the SBM catchment was divided into four periods (Autumn, Snowmelt, Spring and Dry period) according to distinct phases in the hydrograph in order to further analyze the control on stream CO_2 concentration (Figure 3). The stream CO_2 dynamics observed among the different periods were examined visually and any hydrological controls on the CO_2 were identified by the presence and direction of CO_2-discharge hysteresis loops (Evans and Davies, 1998). Similar hysteresis analysis was used to investigate diel patterns in the CO_2 concentration data. Spearman's rank correlation coefficient was used to test for monotonic relationships between the diel amplitude in stream CO_2 concentration and potential drivers.

https://doi.org/10.5194/bg-2019-486
Preprint. Discussion started: 29 January 2020

Correlations were considered significant if $p < 0.05$. The software JMP 14.2.0 (SAS Institute Inc., Cary, NC, USA) was used for all statistical calculations.

3. Results

The mean air temperature and total precipitation for the entire period (Sep 26, 2017-Dec 12, 2018) were 6.8 °C and 704 mm, respectively. The summer and autumn of 2018 were dry with generally low precipitation, the exception was on July 29 with 82 mm rain within 24 hours (Figure 2). Mean and median stream discharge for the open-water period were 30.6 and 0.9 L s^{-1}, respectively, and with a total range from 0 to 668 L s^{-1} (corresponding to a range from 0 to 5.0 mm day^{-1}). However, due to high water table exceeding the range of the pressure transducer the absolute peak discharge occurring during April 5 to April 7 was missed in the measurements. The large skewness between mean and median discharge was an effect of the large number of days without waterflow over the weir during the summer and autumn 2018, 128 days (38%) out of the open-water period. According to frequency analysis, 67% of the days had a mean daily discharge <5 L s^{-1}. Despite the few days with discharge >100 L s^{-1} (7% of the entire period), those days accounted for 69% of the accumulated discharge. The majority (84%) of these high discharge days occurred during the snowmelt in April.

3.1. General CO_2 patterns

The stream CO_2 concentrations during the entire study period (median and mean 3.44 mg C L^{-1} and 3.94 mg C L^{-1}, respectively, corresponding to a pCO_2 of 4778 µatm and 5324 µatm) were highly variable (IQR = 3.26 mg C L^{-1}) (Figure 3) and displayed a bimodal distribution with frequency peaks at ~2.7 mg C L^{-1} and ~6.1 mg C L^{-1} (Figure S3). The lower peak was associated with the snowmelt and spring period, whereas the higher peak was attributed to the autumn period 2017 and to rain events during the dry period of summer/autumn 2018. In addition to the bimodal shape a very distinct peak in frequently measured concentrations was observed at ~1.6 mg C L^{-1}. This peak was attributed to the minimum concentrations values for the diel cycles observed during the spring period.

3.2. Controls on stream CO_2 concentration

The autumn period started dry with low discharge (<3 L s^{-1}) for the initial month of measurements. The CO_2 concentrations were at the same time highly dynamic but unrelated to variations in discharge. The CO_2 concentration reached the maximum

https://doi.org/10.5194/bg-2019-486
Preprint. Discussion started: 29 January 2020

for the autumn (10.89 mg C L^{-1}, which was also the maximum for the entire study period) during late October followed by a decline in CO_2 to ca 2 mg C L^{-1} in early November. During November and December four main rain events were identified which all displayed an increasing stream CO_2 concentration with increasing discharge. In three of these events a positive clock-wise hysteresis loop was observed (Figure 4) where the CO_2 concentration reached its maximum before the discharge did. At the last event during the autumn 2017, the relationship between CO_2 concentration and discharge was close to linear, but still positive. During the snowmelt period the hydrograph was characterized by a diel cycle with melting during day-time resulting in daily discharge peaks which were suppressed during night-time freezing. In contrast to the autumn events the daily discharge peaks were negatively related to the stream CO_2 concentration, and with an anti-clockwise hysteresis loop where the minimum CO_2 concentration was reached before the highest discharge of the event (Figure 5). After the snowmelt discharge peak the spring and early summer periods (late April to early July) were dry with limited precipitation and with a steady decline in runoff (Figure 3). During this period the CO_2 concentration displayed a pronounced diel cycle with daily maximum and minimum CO_2 concentrations reached during early mornings (06:00) and late afternoons (18:00), respectively (Figure 6). The medium amplitude of the diel CO_2 cycle for this period was 2.03 mg C L^{-1}, corresponding to pCO_2 = 2974 µatm (IQR = 1.23 mg C L^{-1}, corresponding to pCO_2 = 2212 µatm), and with the size of the diel CO_2 concentration amplitude being related to both the daily mean water temperature and the shortwave radiation (Figure 7). The diel pattern displayed a clear negative anti-clockwise CO_2-streamwater temperature hysteresis loop, where the median CO_2 concentration could differ up to 75% between day and night-time although being measured at the same stream water temperature (Figure 8).

From early July the stream dried out and hence no runoff over the V-notch weir was generated. During this period the CO_2 sensor was mostly recording an atmospheric signal. However, for five rain events during the summer and early autumn runoff was generated which allowed stream CO_2 determination for shorter periods (Figure 9). During these runoff events (< 2 days long) high CO_2 concentration pulses were recorded (up to 11 mg C L^{-1}). At all events CO_2 was recorded for a longer period than the discharge as the small dam above the v-notch weir was still water-filled for some time after runoff over the weir ceased. Also, common for all events was that the stream CO_2 concentration continued to increase although the discharge peak had passed. During July 29 a heavy rain storm occurred with 82 mm precipitation during 24 hours. Although more than 15%

https://doi.org/10.5194/bg-2019-486
Preprint. Discussion started: 29 January 2020

of the long-term annual mean precipitation fell during one day, low discharge was generated (maximum discharge 6.1 L s^{-1}) due to high evapotranspiration and dry soils (Figures 3 and 9). However, the rainstorm event resulted in close to the highest stream CO_2 concentration (10.81 mg C L^{-1}) being observed during the studied period. As soon as the stream was more permanently refilled in early December and with discharge generated over the weir, the stream CO_2 concentration was back to similarly high levels (typically 5-8 mg C L^{-1}) as observed in the autumn of 2017.

3.3. Sources of DIC

The δ^{13}C-DIC data collected during the falling limb of the spring discharge peak (discharge range 130-9.6 L s^{-1}) were ranging from -13.8 to -12.2‰. This narrow range suggests a relatively constant source of inorganic C during the spring period. Although there was a tendency towards more negative δ^{13}C-DIC values at higher discharge, no significant relationship was found (Figure 10). δ^{13}C-DIC was also unrelated to the stream CO_2 concentration (data not shown).

3.4. Spatial representativeness

The ten streams manually sampled around Uppsala displayed a wide range in CO_2 concentrations (1.8-4.6 mg C L^{-1}) on the day of sampling (June-21 2018), and with the SBM stream (site 3 in table S1) being close to the overall median (SBM, 2.7 mg C L^{-1}; overall median, 3.0 mg C L^{-1}) (Table S1). Furthermore, the CO_2 concentration manually sampled at SBM was close to the sensor recorded CO_2 (2.59 mg C L^{-1}) at the hour of sampling. The SBM stream was also close to the spatial median DOC concentration but slightly elevated in NO_3 and PO_4. The CO_2 concentration was on a spatial scale related to pH but unrelated to catchment area or land-use distribution within the catchment. Furthermore, the CO_2 concentration was on a spatial scale unrelated to open-water mean values of DOC, PO_4 and NO_3, although these variables were sampled during a different period than the CO_2.

4. Discussion

In order to produce large scale estimates of the exchange of GHGs between inland surface waters and the atmosphere, a basic requirement is to know the aqueous concentrations of the gases of interest and how they might vary over time. Headwater streams have been identified as “hotspots” for CO_2 emissions (Raymond et al. 2013; Wallin et al. 2018), but there is limited data capturing the temporal resolution, specifically from streams draining agricultural regions, making large scale

https://doi.org/10.5194/bg-2019-486
Preprint. Discussion started: 29 January 2020

generalizations uncertain. Due to effective drainage, high nutrient conditions and high sun-light exposure (due to zero/limited tree cover), agricultural streams could potentially be very different in their CO_2 dynamics compared with streams draining other environments. Here we continuously measured stream CO_2 concentration in a headwater catchment dominated by agricultural land-use (86%) covering more than one year of the snow-free period. In line with findings from similar studies from other environments (arctic tundra, boreal forest, temperate peatlands, alpine) (e.g. Rocher-Ros et al. 2019; Riml et al. 2019; Crawford et al. 2017; Peter et al. 2014; Dinsmore et al. 2013) we found a mixture of controls on stream CO_2 operating at different time-scales generating a highly dynamic stream CO_2 pattern. These time-scales covers seasonal patterns to diel cycles, or even shorter scales associated to discharge events. Both the magnitude of CO_2 concentrations, and their associated temporal dynamics were found to be high in the current agricultural stream when compared with the literature. The mean CO_2 concentration (3.94 mg C L^{-1} corresponding to a pCO_2 of 5324 µatm) is at the high end when compared with other high-frequency CO_2 data sets covering low-order (<3rd stream order) catchments draining multiple environments, including arctic tundra, boreal forest, hemi-boreal forest, temperate forest, temperate peatlands and alpine areas (typically ranging from ca 0.2 to 6 mg C L^{-1}) (Crawford et al. 2017; Natchimuthu et al. 2017; Peter et al. 2014; Dinsmore et al. 2013). Still, CO_2 concentrations in SBM do not seem to be exceptionally high compared to snapshot-based data from other agricultural streams.

The spatial variability seen in this study, although only based on snapshot samples, and previous studies indicate that CO_2 concentrations in agricultural streams are comparably high (Borges et al. 2018; Bodmer et al., 2016; Sand-Jensen & Staehr, 2012). In addition, the observed temporal dynamics presented here are, to our knowledge, among the most pronounced in the literature, although the number of high-frequency stream CO_2 data sets are limited. For example, the rapid decrease in stream CO_2 during the autumn of 2017, the strong diel cycle (diel amplitude <5.0 mg C L^{-1}) during the spring/early summer period, or the rapid and high CO_2 pulses (<11.0 mg C L^{-1}) occurring in accordance to rain events during the dry late summer/autumn period. These high CO_2 dynamics clearly illustrate the need for continuous high frequency CO_2 concentration measurements in streams in general, and in agricultural streams more specifically. Without such high-frequency data, representative estimates of agricultural stream CO_2 will be associated with high uncertainty. Although based on measurements from a single stream,

https://doi.org/10.5194/bg-2019-486
Preprint. Discussion started: 29 January 2020


Biogeosciences Discussions

these findings in turn indicate that current large-scale stream CO_2 emission estimates, which are largely based on snapshot concentration data with low (or no) resolution in time, might be specifically uncertain for agricultural regions.

According to our continuous data the highly dynamic pattern in stream CO_2 concentration is driven by a complex interplay of hydrology and biology. The high autumn concentrations observed both in 2017 and 2018 are likely an effect of high respiration of organic matter in the stream channel and/or in the adjacent soil water (Figure 3c). This is supported by efficient aquatic microbial DOC degradation (<800 µg C L^{-1} d^{-1}) observed during the autumn period across the ten streams (agricultural land-use, 30-86%) included in the spatial sampling campaign (Peacock et al. unpublished 2019). This should be compared with organic C degradation rates determined in boreal forest and mire streams displaying typically lower rates (<300 µg C L^{-1} d^{-1}, Berggren et al. 2009). The positive CO_2-discharge relationships indicated that event flow pathways, whether those are more surficial or different spatially, were in contact with soils with higher concentrations of CO_2 compared to flow pathways during base flow (Evans & Davies, 1998; Seibert et al., 2009). Also, the clock-wise shape of the hysteresis loop suggests that there is a buildup of CO_2 in the catchment that is flushed out during rain events (Figure 4). The CO_2 pool seems to be limited as the CO_2 concentration drops before the maximum discharge peak occurs, or that vertical patterns in the CO_2 soil profile control the stream CO_2 dependent on dominating flow paths (Evans and Davies, 1998; Öquist et al. 2009). This could explain that the stream CO_2 increase did not reach any source limitation at rain events of lower magnitude (Figure 4d). Similar positive CO_2 concentration-discharge patterns have been observed across different low-order streams (e.g. Crawford et al. 2017; Dinsmore et al. 2013) but the absolute patterns are often concluded to be highly site-specific and even event-specific. Here we suggest, by exploring the hysteresis loops, that such positive relationships are influenced by the size of the available catchment CO_2 pool or the hydrological connectivity to it. In a highly drained low-elevation agricultural landscape where much of the stream runoff is generated through drainage pipes (Castellano et al. 2019), the extent and spatial distribution of these connections between ground- and surface water are central for the CO_2 patterns observed in the stream.

In contrast to the patterns observed during the autumn, during the snow melt period the stream CO_2 was diluted at discharge increases following a diel pattern (Figure 5). The melting and freezing between day and night-time suggests that melt-water

https://doi.org/10.5194/bg-2019-486
Preprint. Discussion started: 29 January 2020

from the surface snowpack during day time to a larger extent reached the stream without picking up an elevated CO_2 signal. Similar dilution patterns in conjunction with snowmelt have been observed in catchments of various land-use but specifically in peatland catchments with limited forest cover (e.g. Wallin et al. 2013). The similarity between this agricultural catchment and open peatlands could potentially be the effect of an efficient melting of the snowpack. Both non-forested peatlands and agricultural fields are open areas subject to direct sunlight, and wind and rain exposure, while the soil under the snow remains frozen. As a result, a large share of the melt-water will never infiltrate the soil but instead reach the surface drainage system as overland flow (Laudon et al. 2007). This is further accompanied by the low hydraulic conductivity of clay soils, which are dominating the catchment of the current study. Although we did not capture the 2-3 days of peak spring flood (due to a water level out of the range of the pressure transducer) it was evident that the stream CO_2 concentration was diluted from ca 6.0 mg C L^{-1} to ca 2.0 mg C L^{-1} during these days, something that is further supported by the similar drop in EC during the peak spring flood from ca 900 to ca 150 µS cm^{-1}. However, as soon as the absolute discharge peak passed, the stream CO_2 concentration recovered rapidly to the pre-peak levels suggesting a shift to hydrological pathways that mobilize a high CO_2 pool, again supported by the concurrent increase in EC. April and May 2018 were characterized by warm and clear weather with an average 4.2°C higher air temperature and 255 more sun hours than the 30-year mean (1961-1990, SMHI). Altogether, this stimulates a kick-start of the aquatic primary production upon snowmelt, which likely explains the steady decline in CO_2 that occurred during late April/early May. During the spring and early summer, a strong diel pattern in CO_2 concentration further developed, likely driven by aquatic primary production consuming CO_2 during day-time. Such diel CO_2 patterns are commonly observed in stream CO_2 time series at base-flow or during receding flow conditions (e.g. Riml et al. 2019; Peter et al. 2014) and are especially pronounced in amplitude in nutrient-rich streams or in streams without canopy shading (Alberts et al. 2017; Crawford et al. 2017; Rocher-Ros et al. 2019). Initial evaluation of the δ^{13}C-DIC data collected during the spring period suggests a relatively steady mixture of geogenic and biogenic DIC although somehow related to variations in discharge (Figure 11). However, given the suppressed stream CO_2 during the spring period, together with the strong diel cycle caused by aquatic primary production, fractionation of a strict biogenic DIC pool (with a δ^{13}C-DIC from -28 to -20‰) could theoretically push the δ^{13}C-DIC towards the less negative values observed in the current study (from -13.8 to -12.2‰) (Campeau et al. 2017b).

https://doi.org/10.5194/bg-2019-486
Preprint. Discussion started: 29 January 2020

Combined studies on aquatic metabolism, C dynamics and stable isotopic composition would further be recommended to disentangle the dynamic CO_2 source patterns in this type of agricultural system.

300

The spring, summer and autumn periods of 2018 were generally dry leading to the stream channel drying out during long periods. The rapid rewetting periods (< 2 days) that occurred following larger precipitation events resulted in high CO_2 pulses (3-11 mg C L^{-1}) generally exceeding the overall median level of stream CO_2 (3.44 mg C L^{-1}) observed during the study period. The intermittent nature of streams, with distinct drying and rewetting episodes, is known to generate high CO_2 concentration 305 pulses and subsequent emissions (Marcé et al. 2019). Such rapid pulses are generally suggested to be a result of intense respiration in the stream bed sediments upon rewetting, or due to a rapid mobilization of terrestrial C, both organic (DOC) and inorganic (CO_2) in connection to precipitation events. However, the findings of high CO_2 pulses upon rewetting have mostly been done in areas that display pronounced dry and wet seasons e.g. Mediterranean areas or Australia (e.g. Gomez-Gener et al. 2015; Looman et al. 2017). Here we show that such stream intermittency can also cause high and rapid CO_2 pulses in a 310 Swedish agricultural setting, highlighting the need for expanding the geographical coverage of studies that investigate stream intermittency in relation to GHG dynamics and emissions. An obvious tool in this work is the use of continuous sensor-based measurements which allow capturing the episodic and unpredictable nature of these phenomena.

5. Conclusions

It is evident from the current study that the stream CO_2 dynamics in an agricultural headwater catchment are highly variable 315 across a variety of different time-scales and with an interplay of hydrological and biological controls. The hydrological control was strong (although with both positive as well as negative influences dependent on season) and rapid in response to rainfall and snowmelt events. However, during growing-season baseflow and receding flow conditions, the aquatic primary production seems to control the stream CO_2 dynamics, which in turn sets the basis for atmospheric emissions. Given the observed high levels of CO_2 and its temporally variable nature, agricultural streams clearly need more attention in order to understand and 320 incorporate these considerable dynamics in large scale extrapolations.

https://doi.org/10.5194/bg-2019-486
Preprint. Discussion started: 29 January 2020

6. Data availability

Data is available from the Uppsala University data repository, LINK WILL BE ADDED

7. Author contribution

MBW and MW brought the idea and designed the study. MBW funded and instrumented the catchment and analysed the data. MW conducted the GIS analysis. JA, MP and ES provided ideas and data. MBW wrote the manuscript with great support from all co-authors.

8. Competing interests

The authors declare that they have no conflict of interest

9. Acknowledgements

Financial support to MBW from the King Carl-Gustaf XVI award for environmental science and from the Finn Malmgren foundation is acknowledged. JA was supported by FORMAS (grant 2015-1559). Jacob Smeds, My Osterman, Philip Johansson and Maud Oger are acknowledged for great support in field and lab.

References

Alberts, J.M., Beaulieu, J.J. and Buffam, I., 2017, Watershed land use and seasonal variation constrain the influence of riparian canopy cover on stream ecosystem metabolism. Ecosystems 20(3), 553-567.

Audet, J., Bastviken, D., Bundschuh, M., Buffam, I., Feckler, A., Klemedtsson, L., Laudon, H., Löfgren, S., Natchimuthu, S., Öquist, M., Peacock, M. and Wallin, M.B. 2019, Forest streams are important sources for nitrous oxide emissions. Global Change Biology, doi:10.1111/gcb.14812

Berggren M., Laudon H., Jansson M., 2009, Hydrological control of organic carbon support for bacterial growth in boreal headwater streams. Microbial Ecology, 57, 170-178. doi:10.1007/s00248-008-9423-6

Bodmer, P., Heinz, M., Pusch, M., Singer, G. and Premke, K., 2016, Carbon dynamics and their link to dissolved organic matter quality across contrasting stream ecosystems. Science of The Total Environment, 553, 574–586.

Borges, A.V., Darchambeau, F., Lambert, T., Bouillon, S., Morana, C., Brouyère, S., Hakoun, V., Jurado, A., Tseng, H.-C., Descy, J.-P. and Roland, F.A.E., 2018, Effects of agricultural land use on fluvial carbon dioxide, methane and nitrous oxide concentrations in a large European river, the Meuse (Belgium). Science of The Total Environment, 610–611, 342–355.

Campeau, A., Bishop, K., Nilsson, M. B., Klemedtsson, L., Laudon, H., Leith, F. I., Öquist, M. G., Wallin, M. B., 2018, Stable carbon isotopes reveal soil-stream DIC linkages in contrasting headwater catchments, Journal of Geophysical Research – Biogeosciences, 123 (1), 149-167, doi:10.1002/2017JG004083

Campeau, A., Bishop K., Billett, M. F., Garnett, M. H., Laudon, H., Leach, J. A., Nilsson, M. B., Öquist, M. G., Wallin, M. B., 2017a, Aquatic export of young dissolved and gaseous carbon from a pristine boreal fen: implications for peat carbon stock stability, Global Change Biology, 23 (12), 5523-5536, doi:10.1111/gcb.13815

Campeau, A., Wallin, M. B., Giesler, R., Löfgren, S., Mörth, C-M., Schiff, S. L., Venkiteswaran, J. J., Bishop, K., 2017b, Multiple sources and sinks of dissolved inorganic carbon across Swedish streams, refocusing the lens of stable C isotopes. Scientific Reports, 7, 9158, doi:10.1038/s41598-017-09049-9

https://doi.org/10.5194/bg-2019-486
Preprint. Discussion started: 29 January 2020

Castellano, M.J., Archontoulis, S.V., Helmers, M.J., Poffenbarger, H.J. and Six, J., 2019, Sustainable intensification of agricultural drainage. Nature Sustainability, 2(10), 914-921.

Crawford, J. T., Stanley, E. H., Dornblaser, M. M., & Striegl, R. G., 2017, CO_2 time series patterns in contrasting headwater streams of North America. Aquatic Sciences, 79(3), 473-486. doi:10.1007/s00027-016-0511-2

Dinsmore, K. J., M. B. Wallin, M. S. Johnson, M. F. Billett, K. Bishop, J. Pumpanen & A. Ojala, 2013. Contrasting CO_2 concentration discharge dynamics in headwater streams: A multi-catchment comparison. Journal of Geophysical Research: Biogeosciences, 118**,** 445-461.

Dinsmore, K. J. & M. F. Billett, 2008, Continuous measurement and modeling of CO_2 losses from a peatland stream during stormflow events. Water Resources Research, 44**,** 11.

Evans, C., Davies, T.D., 1998, Causes of Concentration/Discharge Hysteresis and its Potential as a Tool for Analysis of Episode Hydrochemistry. Water Resources Research 34, 129–137.

Gómez-Gener, L., Obrador, B., von Schiller, D., Marcé, R., Casas-Ruiz, J.P., Proia, L., Acuña, V., Catalán, N., Muñoz, I., Koschorreck, M., 2015. Hot spots for carbon emissions from Mediterranean fluvial networks during summer drought. Biogeochemistry125, 409–426.

Hall Jr, R.O. and Ulseth, A.J., 2019, Gas exchange in streams and rivers. Wiley Interdisciplinary Reviews: Water, p.e1391

Halldin, S., Bergström, H., Gustafsson, D., Dahlgren, L., Hjelm, P., Lundin, L.C., Mellander, P.E., Nord, T., Jansson, P.E., Seibert, J., Ståhli, M., Szilágyi Kishné, A. and Smedman, A.S. (1999) Continuous long-term measurements of soil–plant–atmosphere variables at an agricultural site. Agricultural and Forest Meteorology, 98-99, 75-102.

Holmqvist, M., 1998, Avrinningsdynamik i fem små områden. Vattenbalans, recession, magasinskoefficient och dynamiskt vattenmagasin. MSc thesis, Uppsala University, 54 pp

Hope, D., S. M. Palmer, M. F. Billett, and J. J. Dawson, 2004, Variations in dissolved CO_2 and CH_4 in a first-order stream and catchment: an investigation of soil–stream linkages, Hydrol. processes, 18, 3255-3275.

Hughes, R.M., Herlihy, A.T. and Kaufmann, P.R., 2010, An Evaluation of Qualitative Indexes of Physical Habitat Applied to Agricultural Streams in Ten US States 1. JAWRA Journal of the American Water Resources Association, 46(4), 792-806.

Johnson, M. S., M. F. Billett, K. J. Dinsmore, M. Wallin, K. E. Dyson, and R. S. Jassal, 2010, Direct and continuous measurement of dissolved carbon dioxide in freshwater aquatic systems - methods and applications, Ecohydrology, 3, 68-78, doi:10.1002/eco.95.

Kokic J, Wallin MB, Chmiel HE, Denfeld BA, Sobek S., 2015, Carbon dioxide evasion from headwater systems strongly contributes to the total export of carbon from a small boreal lake catchment. J Geophys Res-Biogeo. 120:13–28. doi:10.1002/2014JG002706

Kokic J, Sahlée E, Sobek S, Vachon D, Wallin MB, 2018, High spatial variability of gas transfer velocity in streams revealed by turbulence measurements, Inland Waters, 8:4, 461-473, doi:10.1080/20442041.2018.1500228

Kyllmar, K., Forsberg, L. S., Andersson, S., & Martensson, K., 2014, Small agricultural monitoring catchments in Sweden representing environmental impact. Agriculture Ecosystems & Environment, 198, 25– 35. doi:10.1016/j.agee.2014.05.016

Laudon, H., V. Sjöblom, I. Buffam, J. Seibert, and M. Mörth, 2007, The role of catchment scale and landscape characteristics for runoff generation of boreal streams, J. Hydrol., 344(3-4), 198-209,

Leith, F. I., Dinsmore, K. J., Wallin, M. B., Billett, M. F., Heal, K. V., Laudon, H., Öquist, M. G., Bishop, K., 2015, Carbon dioxide transport across the hillslope–riparian–stream continuum in a boreal headwater catchment, Biogeosciences, 12, 1881-1892, doi:10.5194/bg-12-1-2015

Linefur, H., Norberg, L., Kyllmar, K., Andersson, S. och Blomberg, M., 2018, Växtnäringsförluster i små jordbruksdominerade avrinningsområden 2016/2017. Uppsala: Sveriges lantbruksuniversitet. (Ekohydrologi, 155).

Looman, A., Maher, D.T., Pendall, E., Bass, A., Santos, I.R., 2017. The carbon dioxide evasion cycle of an intermittent first-order stream: contrasting water–air and soil–air exchange. Biogeochemistry, 132, 87–102.

Natchimuthu, S., Wallin, M. B., Klemedtsson, L., Bastviken, D., 2017, Spatio-temporal patterns of stream methane and carbon dioxide emissions in a hemiboreal catchment in Southwest Sweden, Scientific Reports, 7, 39729, doi:10.1038/srep39729

Osborne, B., Saunders, M., Walmsley, D., Jones, M., Smith, P., 2010, Key questions and uncertainties associated with the assessment of the cropland greenhouse gas balance. Agriculture, Ecosystems & Environment 139, 293–301, doi:10.1016/j.agee.2010.05.009

Osterman, M., 2018, Carbon dioxide in agricultural streams - magnitude and patterns of an understudied atmospheric carbon source, MSc thesis, Uppsala University, 58 pp

https://doi.org/10.5194/bg-2019-486
Preprint. Discussion started: 29 January 2020

Öquist, M. G., M. Wallin, J. Seibert, K. Bishop, and H. Laudon, 2009, Dissolved inorganic carbon export across the soil/stream interface and its fate in a boreal headwater stream, Environmental Science & Technology, 43(19), 7364-7369, doi:10.1021/es900416h.

Peter, H., Singer, G. A., Preiler, C., Chifflard, P., Steniczka, G., & Battin, T. J., 2014, Scales and drivers of temporal pCO_2 dynamics in an Alpine stream. Journal of Geophysical Research: Biogeosciences, 119(6), 1078-1091. doi:10.1002/2013JG002552

Ramankutty, N., Evan, A.T., Monfreda, C. and Foley, J.A., 2008, Farming the planet: 1. Geographic distribution of global agricultural lands in the year 2000. Global Biogeochemical Cycles, 22(1).

Raymond PA, et al. 2013, Global carbon dioxide emissions from inland waters. Nature, 503 (7476), 355-359.

Raymond, P. A., C. J. Zappa, D. Butman, T. L. Bott, J. Potter, P. Mulholland, A. E. Laursen, W. H. Mcdowell & D. Newbold 2012, Scaling the gas transfer velocity and hydraulic geometry in streams and small rivers. Limnology and Oceanography - Fluids and Environments, 2**,** 41-53.

Rhoads, B.L., Schwartz, J.S. and Porter, S., 2003, Stream geomorphology, bank vegetation, and three-dimensional habitat hydraulics for fish in midwestern agricultural streams. Water Resources Research, 39(8).

Riml, J., Campeau, A., Bishop, K., Wallin, M. B., 2019, Spectral decomposition of high-frequency CO_2 concentrations reveals soil-stream linkages, Journal of Geophysical Research – Biogeosciences, doi:10.1029/2018JG004981

Rocher-Ros, G., Sponseller, R.A., Bergström, A.-K., Myrstener, M. and Giesler, R., 2019, Stream metabolism controls diel patterns and evasion of CO2 in Arctic streams. Global Change Biology, doi:10.1111/gcb.14895

Sand-Jensen, K., Staehr, P.A., 2012, CO_2 dynamics along Danish lowland streams: water–air gradients, piston velocities and evasion rates. Biogeochemistry 111, 615–628. doi:10.1007/s10533-011-9696-6

Seibert, J., Grabs, T., Köhler, S., Laudon, H., Winterdahl, M., Bishop, K., 2009, Linking soil- and stream-water chemistry based on a Riparian Flow-Concentration Integration Model. Hydrology and Earth System Sciences 13, 2287–2297. https://doi.org/10.5194/hess-13-2287-2009

Wallin, M. B., Campeau, A., Audet, J., Bastviken, D., Bishop, K., Kokic, J., Laudon, H., Lundin, E., Löfgren, S., Natchimuthu, S., Sobek, S., Teutschbein, C., Weyhenmeyer, G., Grabs, T., 2018, Carbon dioxide and methane emissions of Swedish low-order streams – a national estimate and lessons learnt from more than a decade of observations, Limnology and Oceanography – Letters, 3 (3), 156-167, doi:10.1002/lol2.10061

Wallin, M. B., Grabs, T., Buffam, I., Laudon, H., Ågren, A., Öquist, M. G., Bishop, K., 2013, Evasion of CO_2 from streams – The dominant component of the carbon export through the aquatic conduit in a boreal catchment, Global Change Biology, 19(3), 785-797, doi:10.1111/gcb.12083.

Wallin, M. B., Öquist, M. G., Buffam, I., Billett, M. F., Nisell, J., Bishop, K. H., 2011, Spatiotemporal variability in the gas transfer coefficient (KCO_2) of boreal streams; implications for large scale estimates of CO_2 evasion, Global Biogeochemical Cycles, 25, GB3025, doi:10:1029/2010GB003975

https://doi.org/10.5194/bg-2019-486
Preprint. Discussion started: 29 January 2020

Table 1. Catchment characteristics of the SBM catchment

Catchment area (km^2)	11.3
Elevation range (masl)	13-41
Landuse distribution (%)	
Agricultural land	86
Forest	8
Urban	6
Main Soil type distribution (%)	
Post glacial clay	48
Glacial silt	22
Glacial clay	14
Sandy till	12
Main bedrock distribution (%)	
Granodorite granite	89
Tonalite granodiorite	6
Dacite rhyolite	3
Granite	2

https://doi.org/10.5194/bg-2019-486
Preprint. Discussion started: 29 January 2020

Table 2. Water chemistry at the outlet of the SBM catchment collected during June-November 2017 (n = 8) (Osterman 2018).

	Median	Mean	Min-Max
pH	7.7	7.8	7.4-8.4
EC (µS cm^{-1})	1082	1273	791-1908
NH_4-N (mg L^{-1})	0.10	0.08	0.01-0.1
NO_3-N (mg L^{-1})	0.7	1.9	0.09-6.5
PO_4-P (mg L^{-1})	0.07	0.09	0.01-0.2
DOC (mg L^{-1})	10.0	9.6	4.2-13.1
D.O. (%)	53	62	31-119

445

https://doi.org/10.5194/bg-2019-486
Preprint. Discussion started: 29 January 2020

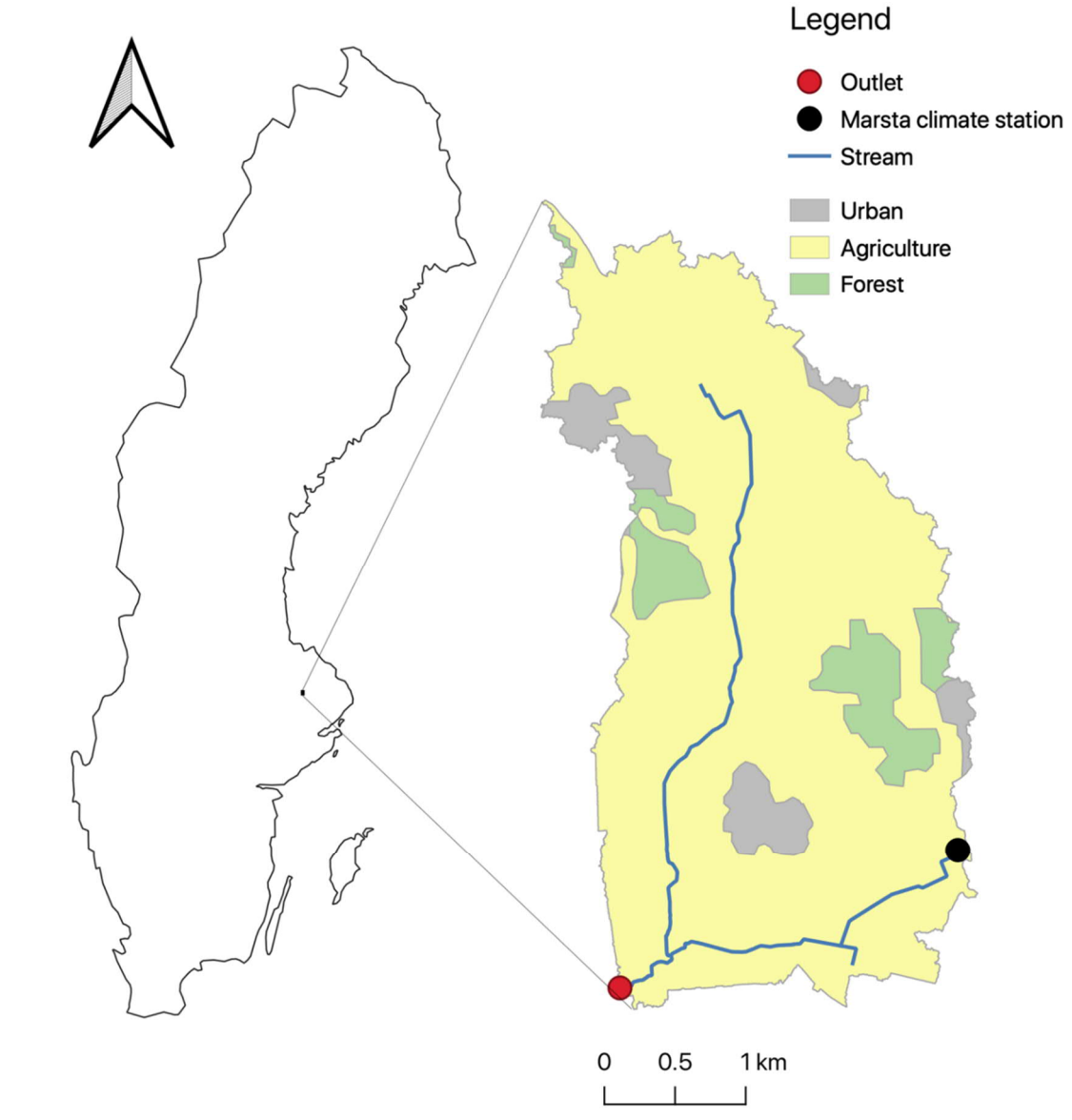

Figure 1. Land use distribution within the SBM catchment (GSD elevation data, grid 2+, ©Swedish Land Survey; CORINE Land Cover 2018, European Environment). The stream-based measurements were conducted at the catchment outlet (red dot) whereas the meteorological data derived from the Marsta Observatory (black dot).

https://doi.org/10.5194/bg-2019-486
Preprint. Discussion started: 29 January 2020

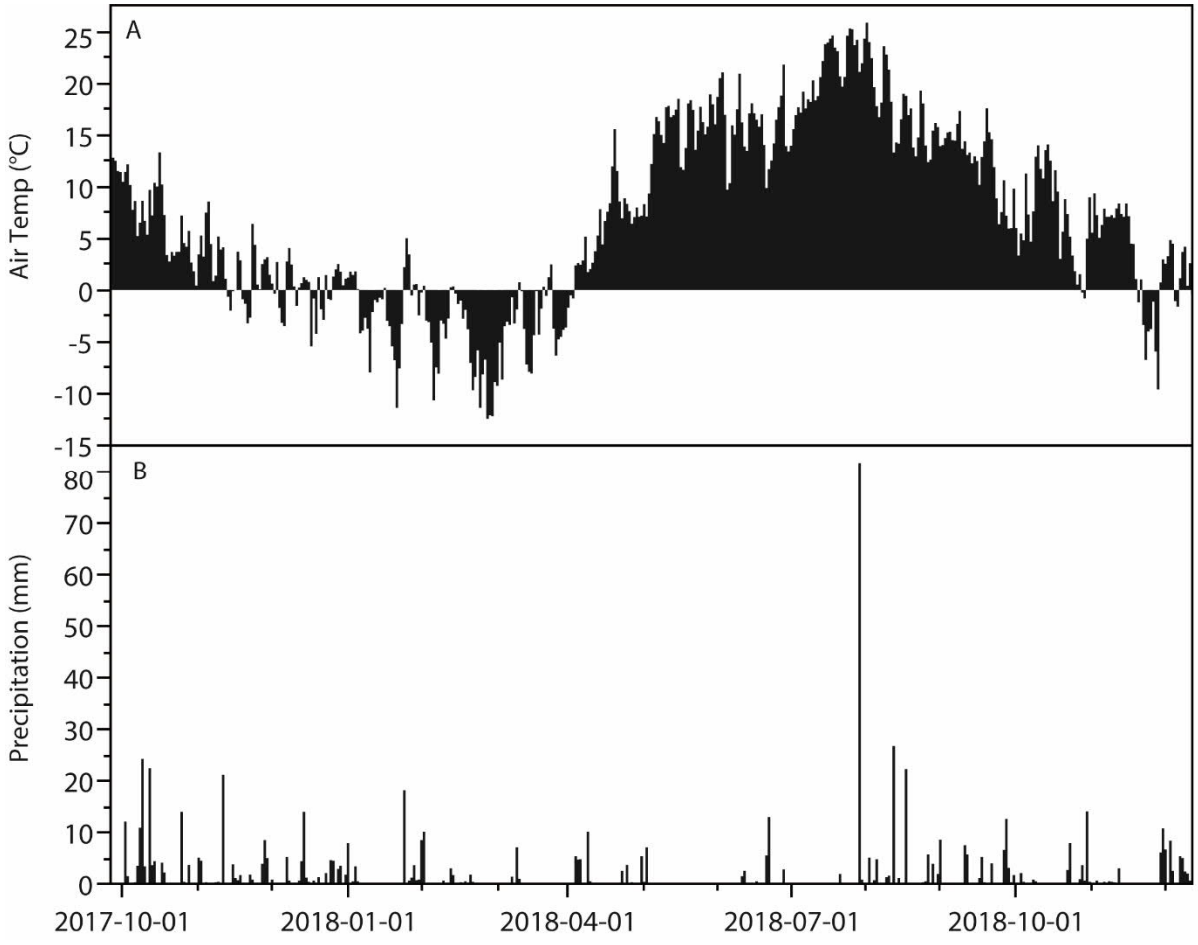

Figure 2. (A) Daily mean air temperature, and (B) daily precipitation during the study period (Sep 26, 2017-Dec 12, 2018) at the Marsta Observatory. Due to malfunctioning sensor the precipitation data for July 29 2018 is collected from the nearby (3 km) SMHI station, Ärna.

https://doi.org/10.5194/bg-2019-486
Preprint. Discussion started: 29 January 2020

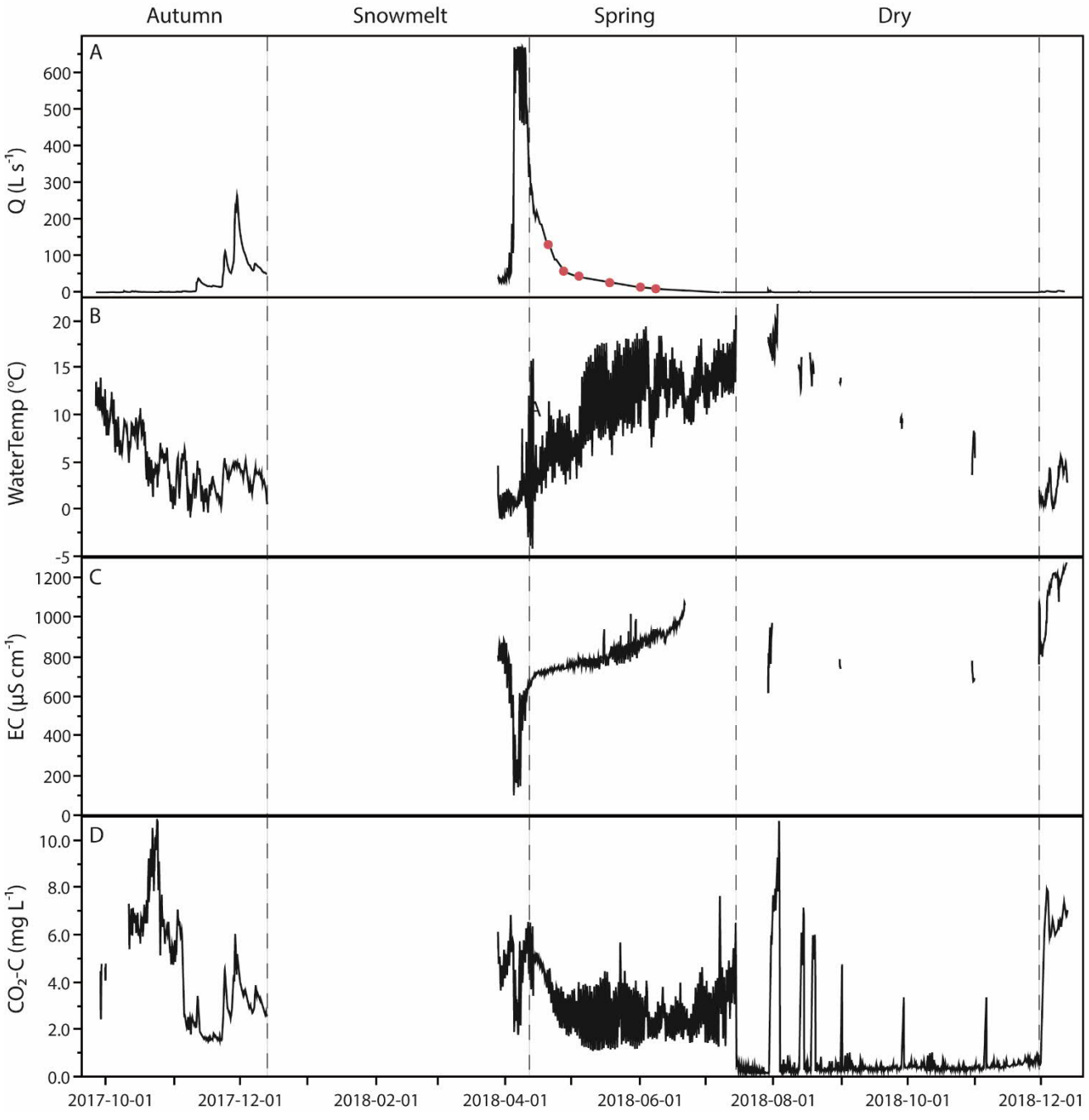

460 **Figure 3. Time series of A) stream discharge (Q) with sampling days for δ^{13}C-DIC highlighted by red dots, B) stream water temperature, C) electrical conductivity (EC), and D) CO_2 concentration for the study period Sep 26, 2017-Dec 12, 2018, with break for the ice- and snow-covered period December-March. The CO_2 data include periods when the sensor was above the water surface during dry periods in summer/autumn of 2018.**

https://doi.org/10.5194/bg-2019-486
Preprint. Discussion started: 29 January 2020

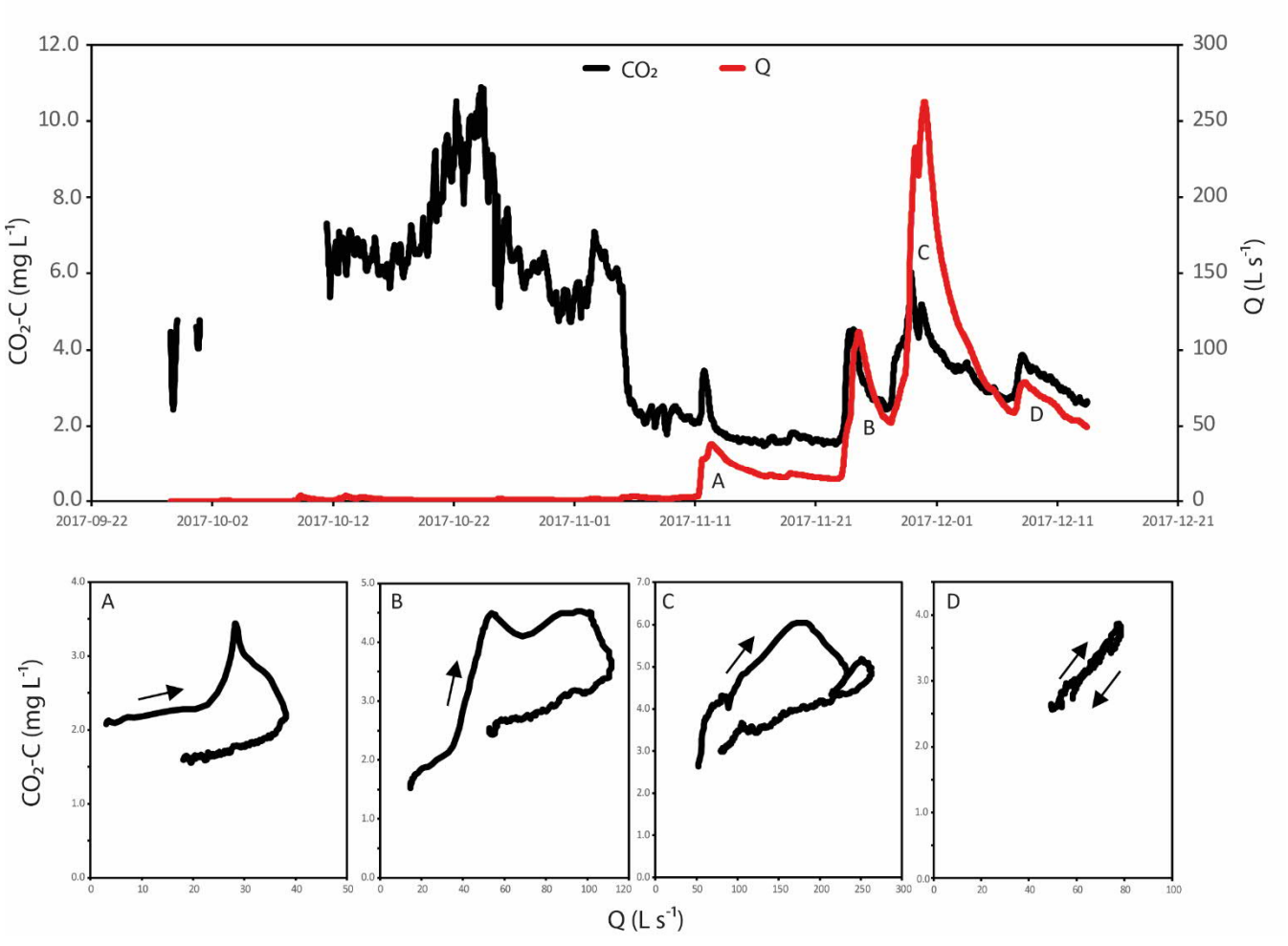

Figure 4. Stream CO_2 concentration (black) and discharge (red) for the autumn 2017 period with CO_2-Q hysteresis plots for four rain events.

https://doi.org/10.5194/bg-2019-486
Preprint. Discussion started: 29 January 2020

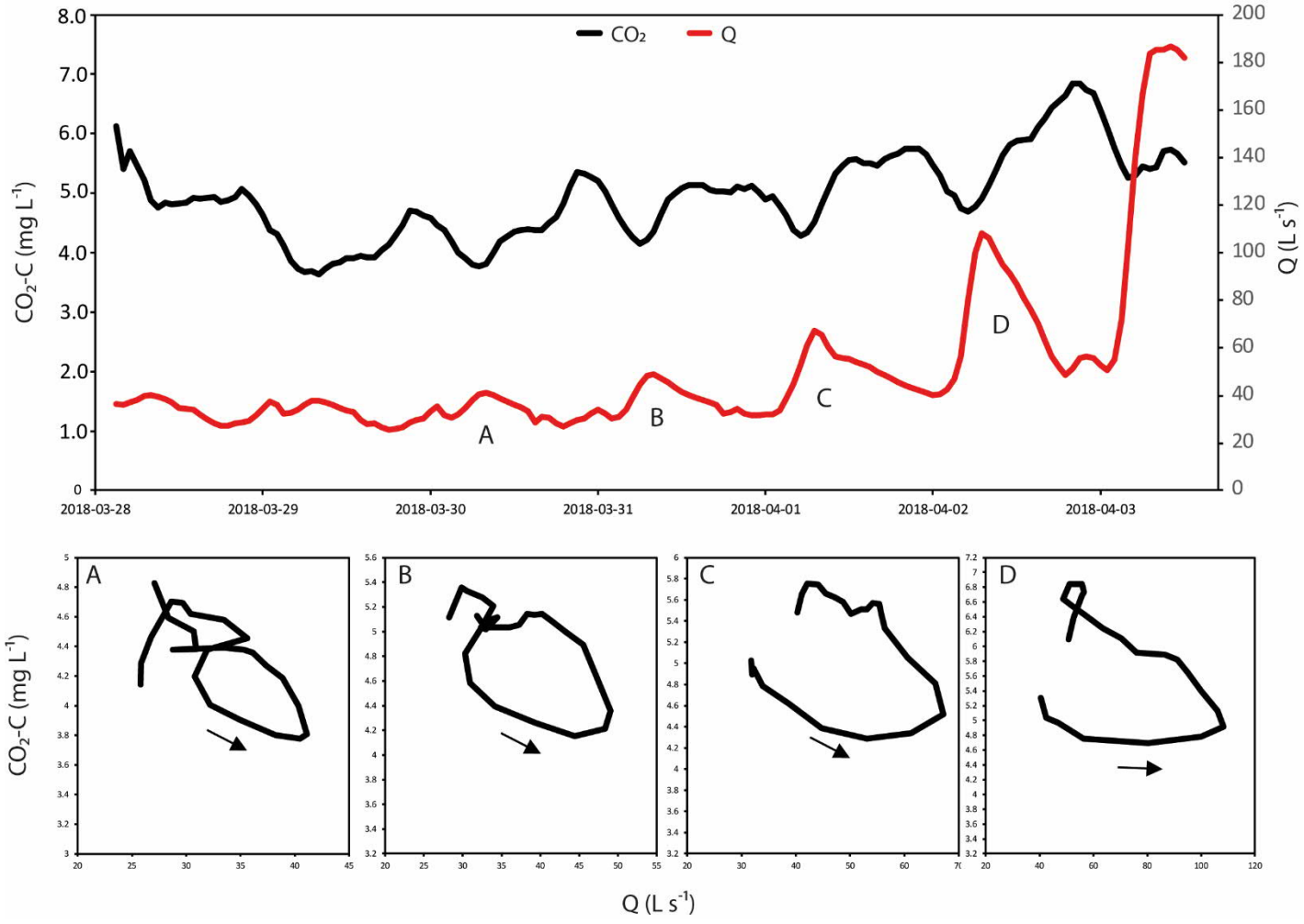

Figure 5. Stream CO_2 concentration (black) and discharge (red) for the snowmelt period 2018 with CO_2-Q hysteresis plots for four discharge events.

https://doi.org/10.5194/bg-2019-486
Preprint. Discussion started: 29 January 2020

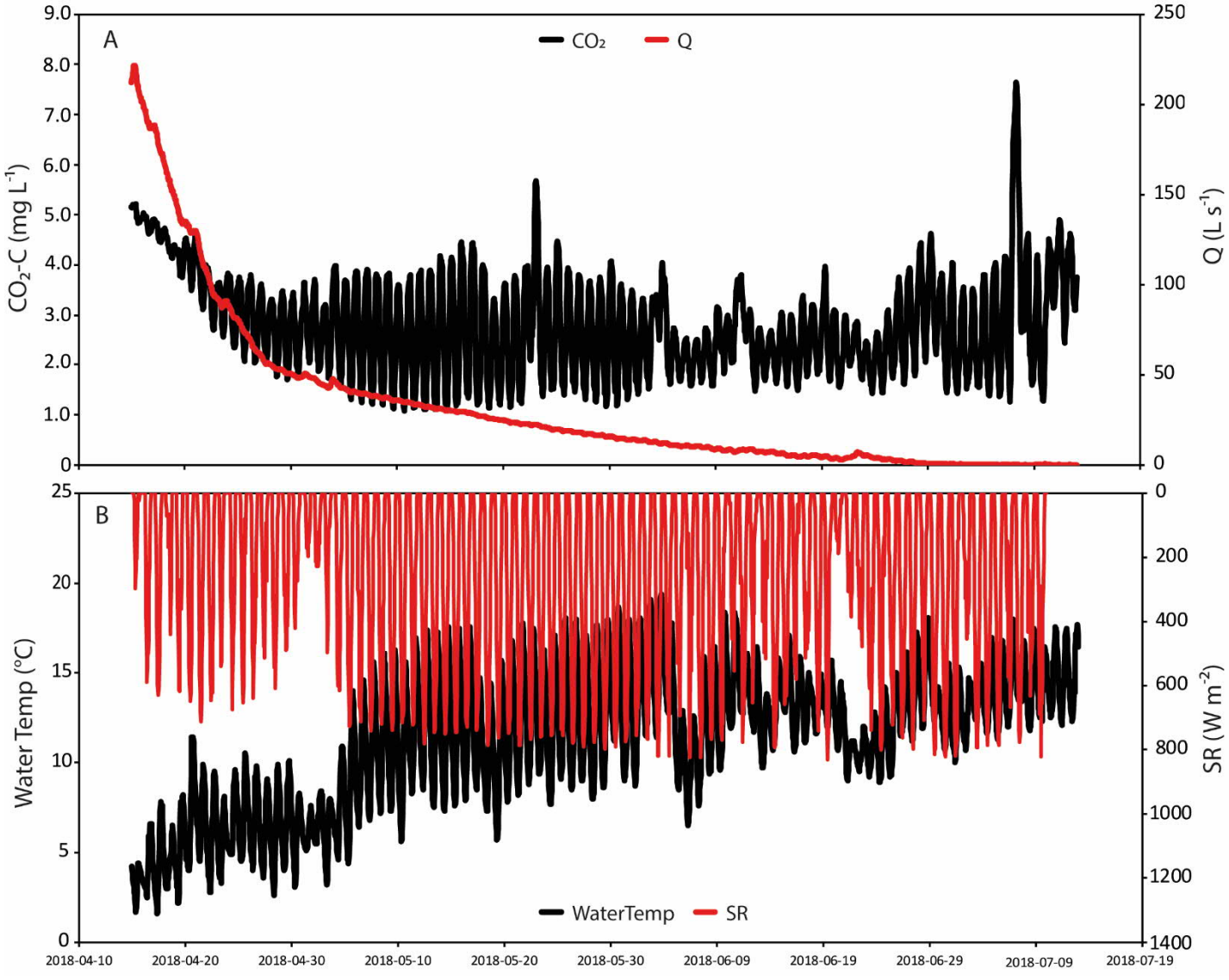

Figure 6. Time series of (A) Stream CO_2 concentration (black) and discharge (red), and (B) water temperature (black) and shortwave incoming radiation (SR, red) covering the period April-July 2018. Note the reverse axis for shortwave incoming radiation.

https://doi.org/10.5194/bg-2019-486
Preprint. Discussion started: 29 January 2020

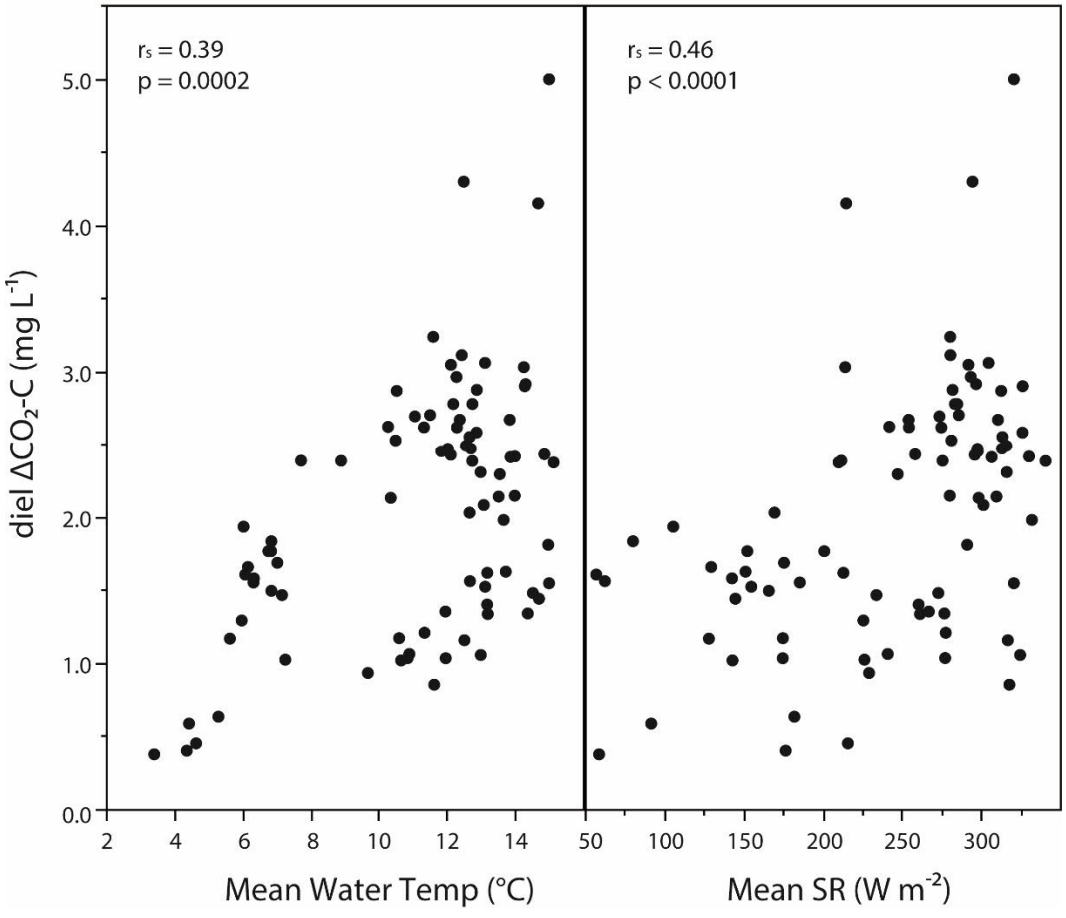

Figure 7. Diel amplitude in stream CO_2 concentration in relation to A) daily mean stream water temperature, and B) daily mean shortwave radiation (SR), covering the period April-July 2018. Statistics are given according to Spearman's rank correlation.

https://doi.org/10.5194/bg-2019-486
Preprint. Discussion started: 29 January 2020

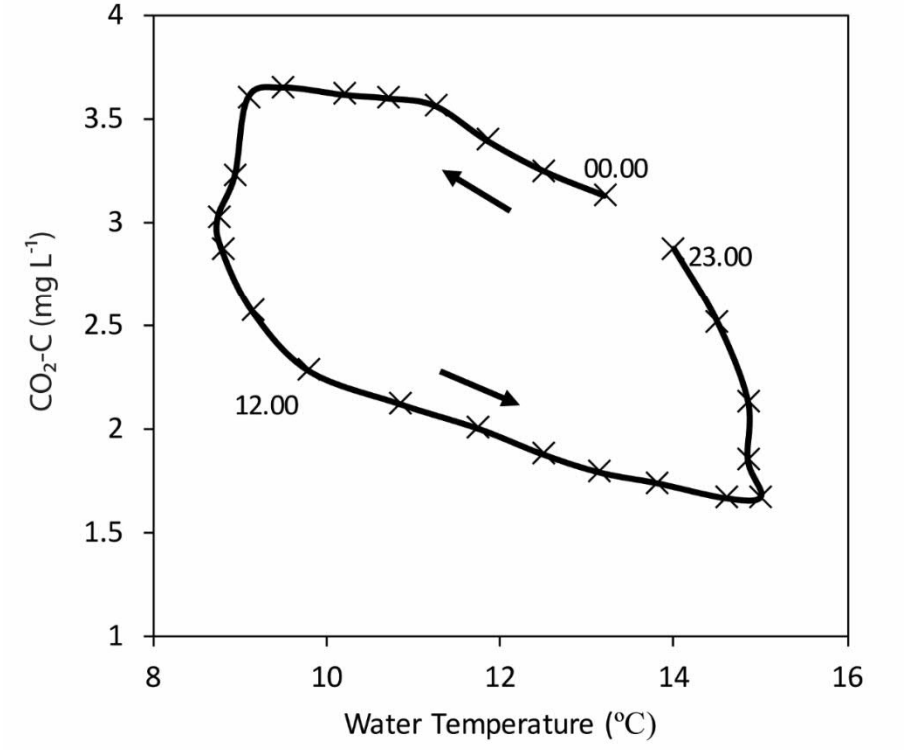

Figure 8. CO_2-Water temperature hysteresis loop based on the median daily values presented in figure 7 covering the period April-July 2018.

https://doi.org/10.5194/bg-2019-486
Preprint. Discussion started: 29 January 2020

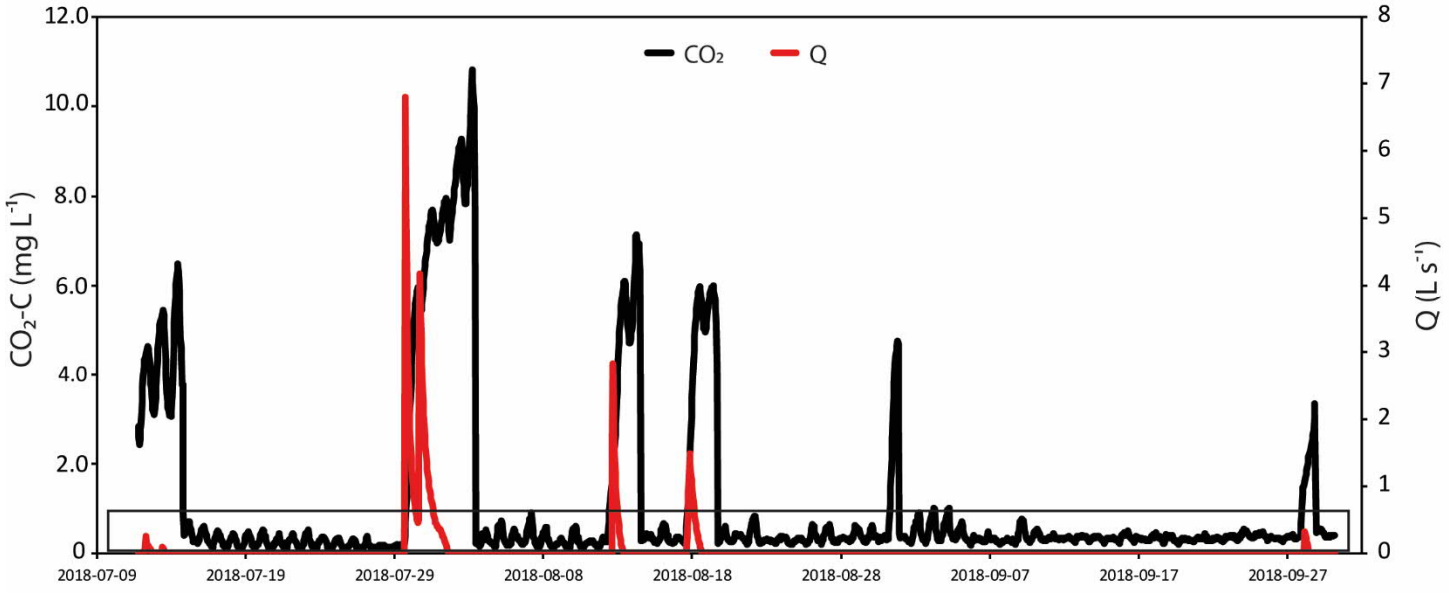

485

Figure 9. Stream CO_2 concentration (black) and discharge (red) for the dry period (July-September 2018). Periods when the CO_2 sensor was above the water table capturing an atmospheric signal (i.e. with concentrations <0.5 mg C L^{-1}) are highlighted by the lower box.

https://doi.org/10.5194/bg-2019-486
Preprint. Discussion started: 29 January 2020

490

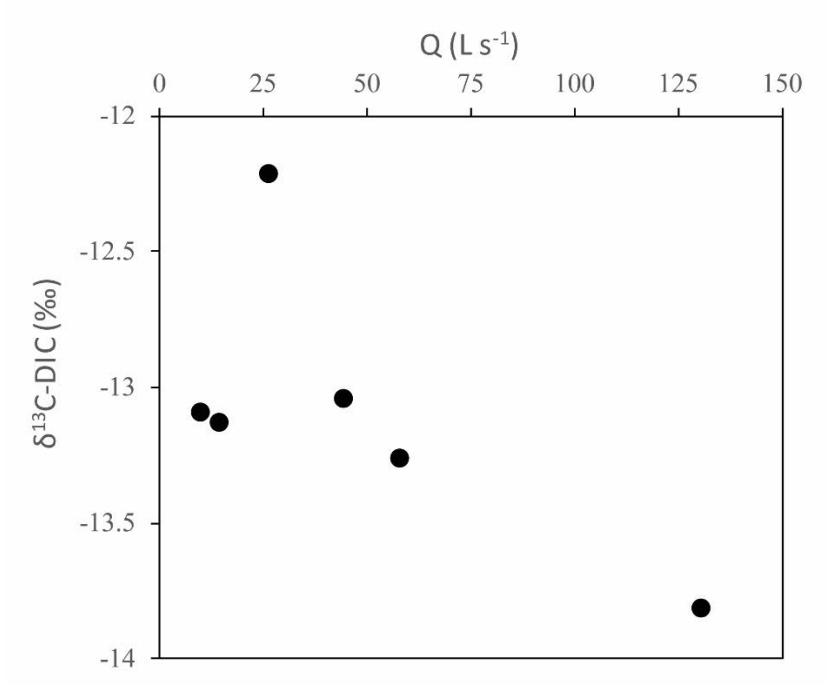

Figure 10. δ^{13}C-DIC as a function of stream discharge. The six sampling occasions covered the falling limb of the snowmelt peak April-June 2018.